

Geodetic Monitoring of Digitally Fabricated Structures Early After Construction

Valens FRANGEZ, Eugenio SERANTONI, and Andreas WIESER, Switzerland

Key words: Digital Fabrication, Engineering Geodesy, Structural Deformation Monitoring

SUMMARY

The construction industry is currently in a process of increased automation and digitization which has an impact on all phases of a building's lifetime, including design, fabrication, assembly, and maintenance. The goal of this innovation is to primarily boost productivity and enhance sustainability. Achieving these goals requires geometrical information about the fabricated objects, first to check for discrepancies between the as-built state and the design one, and second to assess changes over time. Point-cloud based methods, augmented with traditional geodetic metrology are well suited to provide the necessary information. In the current phase of the development, monitoring is particularly relevant because it is necessary to assess the readiness of the innovative fabrication techniques to be adopted by the industry and to assure safety to the users despite the limited experience with the construction processes, designs, and materials used.

Herein we present the geodetic monitoring of three digitally fabricated structures during the early phase after construction, along with the specific challenges and the chosen solutions. The structures are parts of a real building designed and built within the National Centre of Competence in Research Digital Fabrication (NCCR dfab) at ETH Zürich. Concretely, they comprise (i) a curved wall realized by robotically spraying concrete onto a wire mesh previously built in-situ by a robot; (ii) an ultra-thin curved ceiling created using 3D printed formworks, and (iii) a robotically cut and assembled timber beam construction.

Terrestrial laser scanners (TLSs) and a laser tracker (LT) with a hand-guided triangulation scanner were used. The presented deformation analysis consists of point-wise coordinate comparisons within a network, of a cloud-to-mesh (C2M) comparison of pairs of point clouds, and of a hybrid approach denoted as virtual monitoring points (VMP) approach herein, i.e. point-wise analysis derived from the independent registration of small patches of point clouds. The latter is particularly useful for monitoring of structures with salient surface structures where high accuracy is needed but no markers may be applied.

The analyses showed that the structures produced using the 3D printed formwork agree with the plan to within 1.5 cm (maximum C2M deviations). The concrete and the timber structures showed maximum changes of a few mm over the time span of seven months. Using the point-wise LT measurements we found an agreement of deformation patterns with temperature for the curved ceiling.

Geodetic Monitoring of Digitally Fabricated Structures Early After Construction

Valens FRANGEZ, Eugenio SERANTONI, and Andreas WIESER, Switzerland

1. INTRODUCTION

The construction industry is currently undergoing major changes due to automation and digitization in all phases of a building's lifetime. The modernization of construction processes has an effect on design, fabrication, assembly, and maintenance of buildings (Renz et al., 2016). The goal of this innovation is to boost productivity, enhance sustainability, and maintain a high level of resilience (Gifftthaler et al., 2017). Achieving these goals requires geometrical information about the fabricated objects and their changes over time with sufficient spatio-temporal coverage, resolution, and accuracy. Digital fabrication is now at the transition from highly controlled lab environments to real world application, and requires the design, planning, and realization of measurement systems with the appropriate technical characteristics and connection to a well-defined reference frame.

Herein we report about measurement solutions and results from network- and point-cloud-based monitoring of selected digitally fabricated elements installed within a building (DFAB House) in Dübendorf, Switzerland. These elements and the underlying fabrication processes have been developed within the National Centre of Competence in Research: Digital Fabrication (NCCR dfab), an interdisciplinary collaboration involving, among others, architecture, civil engineering, robotics and geodetic engineering. The goals of the monitoring activity were to (i) assess the technological readiness of the respective fabrication processes, (ii) provide data for model and fabrication process adaptations, (iii) enable early detection of potential need for intervention, and (iv) assure safety for the users of the building.

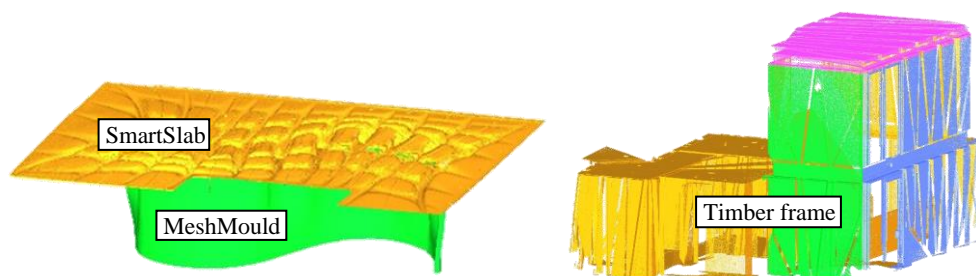


Figure 1: The monitored structures.

The following structures (see Figure 1) have been monitored:

- MeshMould (Hack et al., 2017), an S-shaped wall realized by robotically spraying concrete onto a wire mesh previously built in-situ by a robot
- SmartSlab (Meibodi et al., 2018), an ultra-thin curved ceiling, created from 11 segments, prefabricated using 3D printed formworks, assembled on site using post-tension cables and resting on top of MeshMould
- timber frame (Toma et al., 2018), a robotically cut and assembled timber beam construction which rests directly on top of SmartSlab and MeshMould

For all these structures, the deviations of the as-built state from the designed state and changes over time had to be determined. Particular challenges for the monitoring over time were the missing knowledge about the magnitude and location of the expected deformations, the absence of parts known to be stable, and the very limited permission to establish point markers for the duration of the project. We have chosen to cope with these challenges by using very high accuracy geodetic network measurements with a laser tracker (LT) and 3D laser scanning with terrestrial laser scanners (TLSs) as basis for the monitoring which was carried out over a duration of seven months starting shortly after construction. Laser scans obtained within the first month after the installation of the respective structures were used to assess the deviations from the design resulting from the fabrication process, transport, and assembly.

The remainder of the paper is structured as follows: section 2 contains a brief general overview of the applied monitoring methods; the data acquisition, including used instruments and measurement setups, is presented in section 3, and we discuss the results in section 4. The paper concludes with a short summary.

2. DEFORMATION MONITORING

Geodetic monitoring is one of the key tasks of engineering geodesy, and its goal is to perform a statistically corroborated identification and quantification of geometric changes (Kuhlmann et al., 2014). Depending on the application and the desired outcomes, the monitoring can be performed using point-wise or areal measurements. We apply both approaches in this paper. Network measurements using a LT provide highly accurate point-wise information, and 3D laser scanning yields less accurate but areal information; the two are thus complementary. For economic and technical reasons these solutions are primarily suited for epoch-wise rather than temporally continuous measurements, therefore we acquire the state of the structures herein at discrete epochs and analyse the changes between pairs of epochs.

The selection of appropriate time intervals between the measurement epochs requires knowledge of the motion pattern of the object of interest in terms of magnitudes, periodicity, etc. (Heunecke et al., 2013). This hold for all epoch-wise monitoring methods. Herein, there was only limited knowledge about the deformation patterns to be expected, which would suggest to start with short time intervals and possibly adapt them over time. However, since the main goals were here on quantifying the deviations from the design and relevant changes of these deviations were expected to build up only over longer time spans, intervals of several weeks were chosen.

2.1 Network-Based Deformation Monitoring

Network-based deformation monitoring is a very well established approach, see e.g. Pelzer (1979), Niemeier (1985), Caspary (2000), Heunecke et al. (2013). If it is carried out according to the method of strict analysis within a congruency model, it is particularly useful in classifying the network points into stable and unstable points and allows the implicit definition of the coordinate system using only the stable points. Herein we could not apply this approach because only the SpatialAnalyser (SA) software (NRK, 2020) was available for processing the LT measurements, and it was not possible to connect the measurements inside the building to stable reference points inside or outside the building. So the coordinate system was instead defined by assuming that a specific subset of the marked points within the building were stable on average; the analysis is thus a relative analysis and not an absolute one.

2.2 Areal Deformation Monitoring

Instead of representing an object of interest by a group of carefully selected and marked discrete points, the object's surface can be represented by a point cloud with high spatial resolution, i.e. points densely covering the surface (Tsakiri et al., 2006). Deformations can then be quantified by analysing point clouds obtained at different times. Such TLS-based monitoring has already found widespread application, e.g. for monitoring of dams (Eling, 2009), tunnels (Van Gosliga, 2006), and bridges (Paffenholz and Wujanz, 2019). An overview about modelling strategies and challenges for areal deformation monitoring is given by Neuner et al. (2016), and Wunderlich et al. (2016). Established approaches for the calculation of differences between point clouds are cloud to cloud (C2C), cloud to mesh (C2M), or mesh to mesh (M2M) comparisons (Barnhart and Crosby, 2013). The result is often a deviation map, colour-coded with the magnitudes of geometrical differences between the two datasets.

For the analysis the point clouds need to be transformed into the same coordinate system. This so-called registration can be achieved either using special targets placed within the scanned scene, or using just the point clouds and transforming them such that the distances between the point clouds are minimized. The latter is typically achieved using the iterative closest point (ICP) algorithm introduced by Besl and McKay (1992), and Chen and Medioni (1991), or a variant thereof. Only stable parts of the point clouds should be used for registration. Friedli and Wieser (2016) have presented an approach that identifies stable areas automatically within the target-less registration process.

2.3 Virtual Monitoring Point Approach

We introduce also a hybrid approach using point cloud data to obtain local, quasi point-wise displacements. We denote it as virtual monitoring point (VMP) approach. The underlying idea is to select small (source) patches – in the present application case covering only a few cm^2 – from one of the point clouds to be compared, and calculate the transformation yielding a best fit between this patch and the corresponding part in the other point cloud. Any point within the source patch can then be selected as VMP, because the transformation parameters allow calculating the corresponding point in the other point cloud, and thus the displacement between the epochs. Herein, we define the source patches manually in one point cloud, use ICP to calculate the respective transformation parameters, and we use the centroid (centre of gravity) of each patch as the corresponding VMP. A similar approach was also presented by Raffl (2019). However the authors use full point clouds in that case and do not partition them in smaller patches.

This approach is especially suitable for monitoring where high precision is required but marking points for network (or high precision polar) measurement is not possible. In the present project this was the case with SmartSlab. A prerequisite is that the surface has sufficient structure to facilitate the patch-wise registration.

3. DATA ACQUISITION

The measurements were carried out over the duration of seven months in epochs, approximately one-month apart except for one interval which was three months. Table 1 shows the epochs and the structures measured respectively. For practical reasons not all structures could be scanned at all epochs, and the LT measurements only started in the third epoch.

Three of the instruments used for the data acquisition are shown in Figure 2. All instruments have been calibrated by the respective manufacturer prior to the start of the monitoring project. Indoor temperature values were available for the last three months (see Table 2). More details on the techniques, the measurement setup, and environment are given in the following sections.

Table 1: Measurement epochs and employed techniques. LT = laser tracker; LS = laser scanning.

Structure (technique)	Epoch (date and name)						
	19.12.18 EP1	9.1.19 EP2	14.4.19 EP3	24.4.19 EP4	15.5.19 EP5	12.6.19 EP6	4.7.19 EP7
SmartSlab, MeshMould (LT)			X	X	X	X	X
Timber frame (LT)			X	X	X	X	X
SmartSlab, MeshMould (LS)	X	X		X		X	X
Timber frame (LS)					X	X	X

Table 2: Average indoor air temperature over the five hours prior to the start of the measurements, and temperature differences between subsequent epochs. No temperature data are available for EP1 and EP2.

Epoch	EP3	EP4	EP5	EP6	EP7
T [°C]	23.7	26.4	23.5	22.2	26.7
ΔT [K]	/	2.7	-2.9	-1.3	4.5

3.1 Geodetic Network Measurements

The Leica Absolute Tracker AT960-XR was used together with its accessories, i.e. the Absolute Scanner LAS and several reflectors, for the point-wise measurements and the VMP approach. The specified accuracy of the LT is $15 \mu\text{m} + 6 \mu\text{m}/\text{m}$ (2σ) per coordinate when it measures to reflectors and $60 \mu\text{m}$ (2σ) when scanning (Leica, 2017a). SA was used to control the acquisition process.



Figure 2: LT Leica AT960-XR during measurements (far left), Leica Absolute Scanner LAS during use (left), LS Leica P50 during scanning process (right), and laser scanning target installed in the SmartSlab module (far right).

A point measured by the LT is materialized by a target. Two types of spherically mounted retro-reflectors (SMRs) were used herein, namely reflectors for fixed installations (RFIs) which are glass reflectors, and red ring reflectors (RRRs) which are corner cube reflectors (CCRs). The RFIs are specially designed for network measurements. They are usually mounted directly onto the measuring object using hot glue without any special centering. The CCRs, on the other

hand, are moved between points. Herein we used them for inter-epoch registration by placing them temporarily in reflector holders, which were fixed to the structure. In our case, this was done at horizontal surfaces such that only a strong double-sided tape was needed for fixing the reflector holders. In total, there were 20 RFIs (point IDs O) and four reflector holders (point IDs P) for four CCRs, mounted on the SmartSlab and timber frame structures quasi permanently, i.e. for the duration of the monitoring project (see Figure 3).

Since SmartSlab and timber frame are on different floors, the assembly of points represents two separate networks, namely the SmartSlab and the timber frame network, each with its own local coordinate system. The origin of the coordinate system is in both cases placed in a corner of the room, and the coordinate axes are oriented as shown in the figures. Figure 3 also shows the LT locations S1, S2, and S3 and the lines of sight between the LT and the monitoring points. Four RFIs (O3, O6, O9, and O12) in the SmartSlab network are attached to the top of MeshMould (S-sh-shape in the figure). We considered them stable on average and used them for establishing the coordinate system for the point-wise analysis. All other RFIs in this network are attached to the ceiling and are considered instable object points. In the timber frame network, all RFIs except O21 and O22 lie on top of horizontal beams, see also Figure 4.

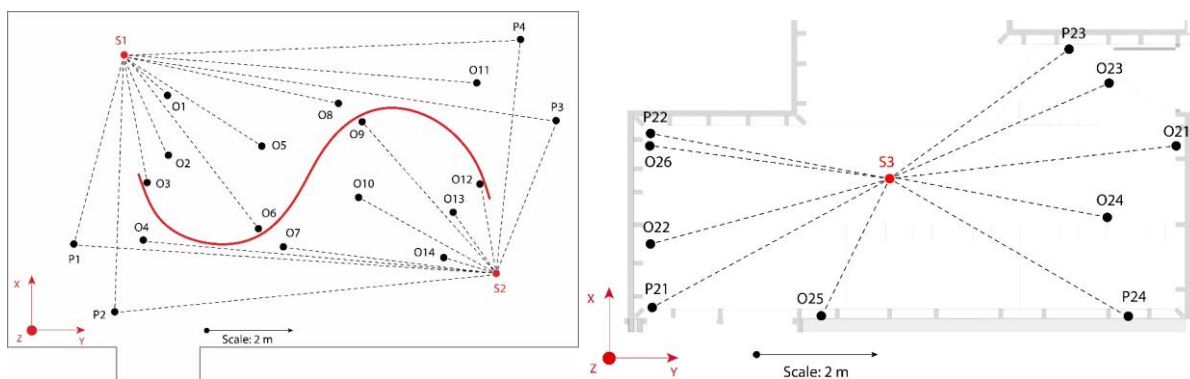


Figure 3: Lines of sight between the LT and the network points for SmartSlab (left) and timber frame (right) measurements.

The signal propagation through glass in the case of the RFIs introduces systematic deviations of the calculated coordinates because of the beam deflection at the air-glass interface. The effect depends on the angle of incidence and is negligible for deformation monitoring if the relative location orientation between tracker and reflector hardly changes over time. No such effect occurs for the CCRs. The effect for reflectors at the distance of 2 m (the closest point in the network) is negligible, if the instrument is positioned at the same locations in each epoch within a centimetre; it is even less for greater distances. Consequently, we paid attention to positioning the tracker at the same location and instrument height for each epoch within that accuracy, which increased the effort for the field work but was feasible.

The network acquisition process took about two hours, excluding the prior warm-up of the instrument, which lasts three hours. The warm-up is necessary in order to homogenize the temperature within the instrument and thus reach the specified accuracy.



Figure 4: Timber frame network point locations.

3.2 Laser Scanning

Two laser scanners, a Z+F Imager 5016 and a Leica P50, were used to scan the structures. They have similar accuracy specifications with range noise below 1.2 mm (2σ) (Leica, 2017b; Z+F, 2017) and negligible angular noise for the present distances of up to about 8 m. Using different scanners was necessary because of the scanner availability. At each epoch only one of the scanners was used. A total of 13 scanning locations for SmartSlab and four for timber frame were needed per epoch. The acquisition process took about three hours per epoch with the chosen scan settings (highest quality and normal resolution, i.e. average point spacing of 3.1 mm at 10 m). The instrument setup locations were repeated within a few dm in each of the epochs.

Paper black and white checkerboard targets were placed in the scanned areas for the inter- and intra-epoch registrations. In both SmartSlab and timber frame, four of them were placed quasi permanently (for the duration of the monitoring project, see Figure 2) and another 20 of them temporarily (removed after each epoch). The need for so many targets was due to several obstructions impairing the overlap between scans from different setups. We placed the targets on the floor and at various heights on the walls to strengthen the geometric configuration for the registration. The inter-epoch registrations have been conducted using scanner proprietary software with all the available targets within each scene. This yielded a registration accuracy of about 2 mm (2σ , as reported by the software). ICP-based, i.e. target-less, intra-epoch registration did not yield sufficiently accurate results in this setting. The reason is the combination of nearly feature-less areas, little overlap between the scans, and significant point-cloud differences in the overlapping regions due to mixed pixels and obstructions resulting from the many edges of the SmartSlab. On the other hand, for the inter-epoch registration, the permanently mounted TLS targets were found not to be stable enough whereas ICP-base registration using the floor and the S-shaped MeshMould structure worked well.

Small areas of the SmartSlab surface were also scanned using the Absolute Scanner LAS, which is a hand-guided triangulation scanner tracked by the LT. The resulting points have a very high point density (acquisition with 150'000 points / sec), sub-mm accuracy, and are georeferenced with respect to the LT. These data were intended for use with the VMP approach.

4. RESULTS

4.1 Network Data

The coordinates of the network points were estimated independently for each epoch using SA. The coordinate system was thereby defined by points considered stable on average, i.e. points

O3, O6, O9, and O12 for the SmartSlab network and points P21, P22, P23, and P24 for timber frame. After transformation of the network onto these reference points, the deformation analysis consisted in the calculation of the coordinate differences between subsequent epochs, their visualization, and assessment. The displacement vectors are shown in Figure 5 and Figure 8, for SmartSlab and timber frame respectively, and separately for the horizontal and the vertical components.

The maximum recorded displacements between subsequent epochs in the SmartSlab network are 0.35 mm for the horizontal components (O11) and 0.37 mm for the vertical ones (O1), both between EP4 and EP5. These two points are located in the part of the structure that is the most exposed to the exterior, as it is surrounded by windows.

In general, the biggest horizontal movements occurred among point groups O1 – O4 and O11 – O14. For the duration of the monitoring project, the maximum horizontal displacements of the network points (between any two epochs) were 0.35 mm (for O11 and epochs EP4 and EP5). The pattern shows that these two groups of points either moved away from or close to each other during the same time periods. This can be interpreted to a large degree by thermal expansion, as will be further corroborated using an analysis of the distances between the network points. The height displacements, are predominantly in a downward direction indicating a settling of the ceiling relative to the top of MeshMould (reference points). The maximum vertical displacements found over the duration of the project were 0.38 mm (for O1 and epochs EP4 and EP5).

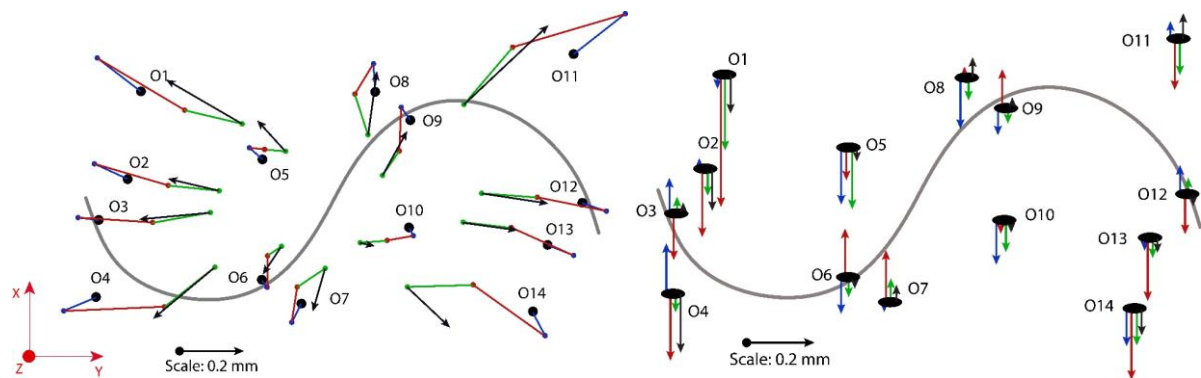


Figure 5: Horizontal (left) and vertical (right) displacement vectors for the SmartSlab network points.

In order to better understand the potential dependence of the SmartSlab deformations in relation to temperature, 3D distances for all point pairs within each epoch were computed and then analysed over time. As an example the pair-wise distances are shown in Figure 6 (left), and the scale values calculated from these distances and the distance changes between epochs are shown in Figure 6 (right) for each pair of points between EP1 and EP3, as an example. The figure already indicates a fairly consistent scale of about -35 ppm for the longer distances; with short distances, the scale estimation is affected more by measurement noise and should thus be interpreted only with care.

The scale change values for each epoch in relation to EP1 are shown in Figure 7 as a function of the temperature changes relative to EP1. Linear regression taking only point pairs with a distance greater than 4 m into account indicates a scale of approximately 19 ppm/K. While the value does not strictly correspond to the typically assumed 10-13 ppm/K of concrete, it still

indicates a thermal expansion of SmartSlab resulting in sub-mm changes of the dimensions. Further investigations are necessary to clarify which other factors affect the structure beyond the temperature changes.

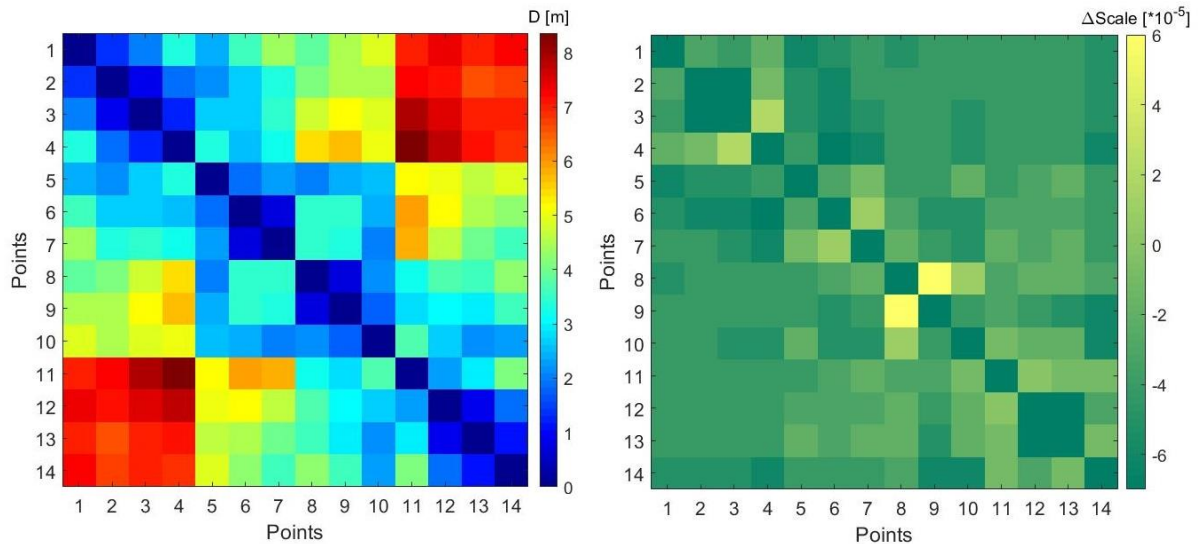


Figure 6: Pair-wise distances (left) and scale (right) changes in between epochs EP1 and EP3 (SmartSlab network).

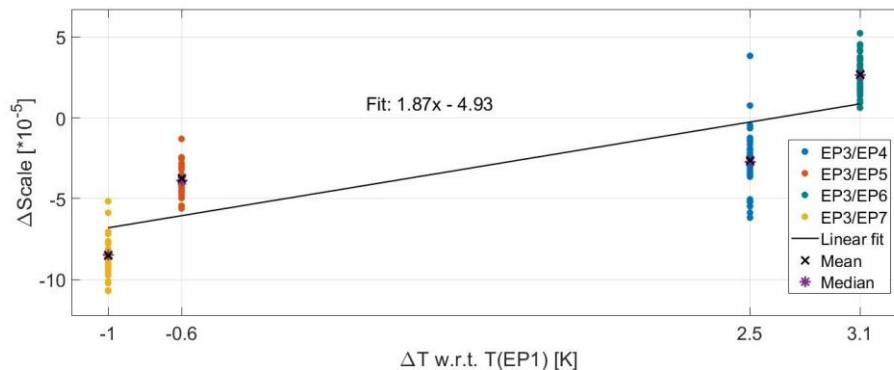


Figure 7: A linear relation of temperature change vs. scale change using distances longer than 4 m from all four epoch datasets (SmartSlab network).

The timber frame network point displacements are bigger than those observed in the SmartSlab network. Horizontal displacements were the biggest at point O25, which moved about 0.93 mm between epochs EP6 and EP7. Its height changed by 0.41 mm between the same epochs. The reason could be the impact of external environmental changes since this point is located on the outer wall of the structure. As opposed to the SmartSlab network the coordinate changes within timber frame do not show a clear and easily interpretable pattern, although points O21, O23, O24, and P23 exhibit a similar pattern of apparently almost circular movement. Again the patterns are likely related to changes of environmental parameters, in this case probably primarily humidity. However, a more in depth interpretation requires structural expertise and tools for modelling the geometrically complex timber structure.

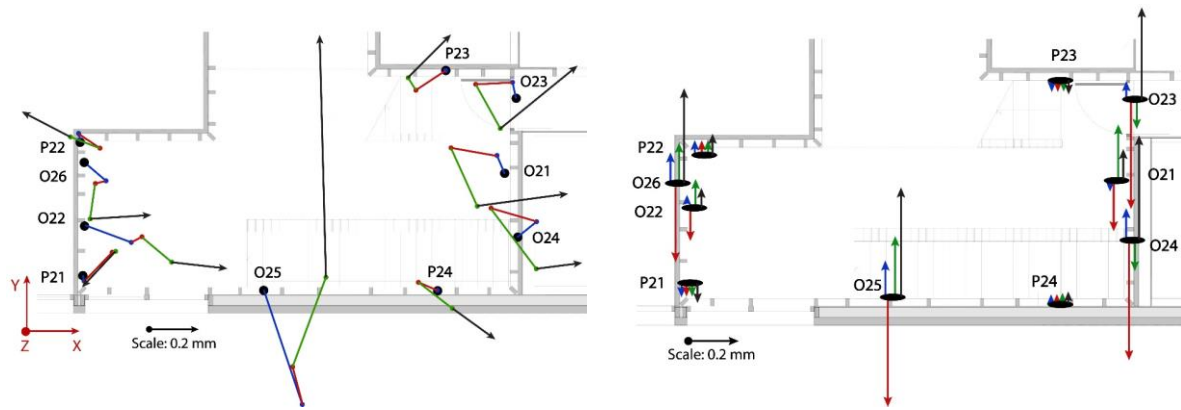


Figure 8: Horizontal (left) and vertical (right) displacement vectors for timber frame network points.

4.2 Point Cloud Data

The TLS point clouds facilitated the comparison of the as-built state to the designed state (CAD model) of the SmartSlab. The C2M deviations are shown in Figure 9 (left). The shown deviations result from deviations during segment fabrication (e.g. potentially deviations of the formwork assembly), but also deviations resulting from the on-site assembly of the ceiling, the post-tensioning contributions and from concrete creeping. Positive values of deviations correspond to the as-built state being higher than the planned, while the blue areas indicate vice versa. A discontinuity of the deviation pattern between distinct segments can be seen in several cases, e.g. between segments 5 and 6. The maximum differences are on the level of ± 1 cm.

The displacement map of SmartSlab generated when comparing EP1 and EP7 in the vertical direction is shown in Figure 9 (right). These two epochs were chosen to be included in this paper since they are timely the farthest apart and show the largest changes. The deformations over the period of about seven months are on the level of a few mm, mostly below 4 mm. The maximum negative displacement, indicating settling, is seen on the very left and very right parts of the structure. Since the support of SmartSlab is only in the middle of it, i.e. by the MeshMould, the observed behaviour qualitatively fits the expectations. There are also parts that have slightly increased in height, i.e. middle of the structure between 2 mm and 3.5 mm. This behaviour cannot be explained without better understanding of the structure itself.

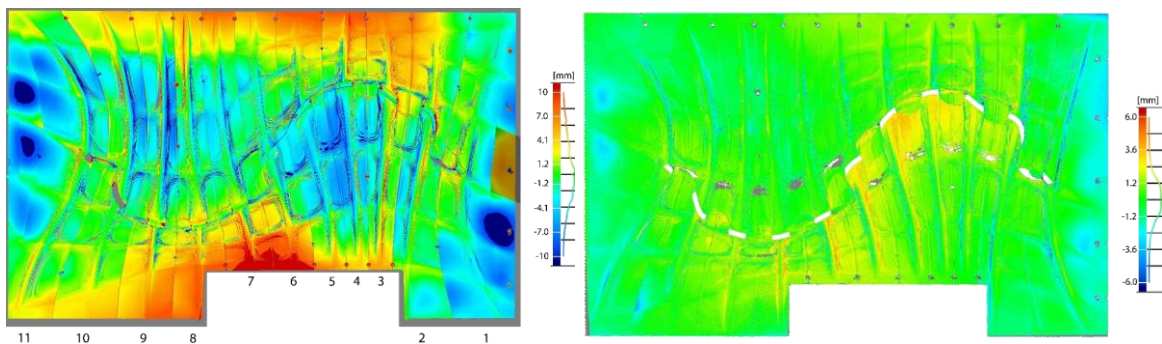


Figure 9: Deviation map when comparing the CAD model (provided by ITA, ETH) with EP1 with segment numbers (left) and displacement map of SmartSlab generated after comparing two epochs seven months apart (right).

Displacement maps for the timber frame structure are shown in Figure 10. We conclude that there were no significant vertical changes over the period of two months (i.e., the period over

which scans of the timber frame were possible) which could be detected using TLS. All the displacements occur within ± 1.2 mm and are thus at or even below the scanner's noise level. Concerning the outer wall, it can be observed that there are areas which reach inwards displacements of up to 1.5 mm. The opposite behaviour can be observed for the inner wall, where outward displacements of about 1.5 mm have been recorded. This is especially visible for the flat panels behind the timber beams; an analysis of the relative deformations of the timber beams and these panels has not yet been carried out. No particular differences can be seen between individual modules of the timber frame, indicating the whole structure behaves quite uniformly. For both cases, SmartSlab and timber frame, the results selected for display herein are representative of all pair-wise analyses carried out.

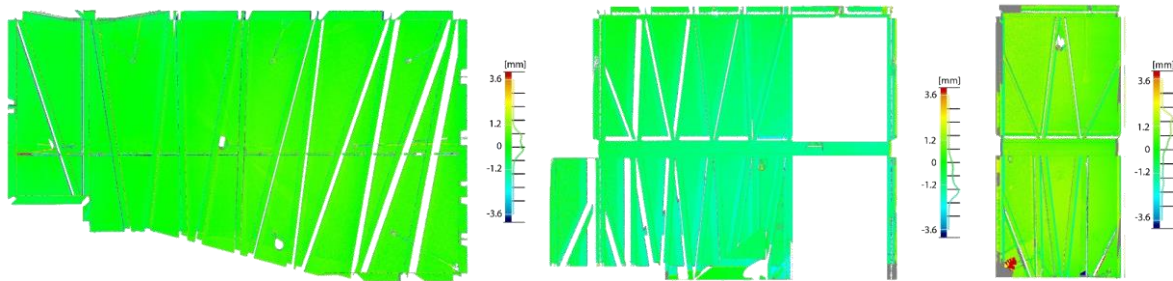


Figure 10: Displacement maps of timber frame when comparing EP5 and EP7 ceiling (left), outer (centre), and inner wall (left).

4.3 Virtual Monitoring Point Data

Due to a technical problem, the data originally collected on site for the VMP approach could not be analysed. Instead, the feasibility of the approach was briefly investigated in a separate experiment using a sample of a separately fabricated part of the SmartSlab structure (see Figure 11). This also allowed introducing significant displacement and providing ground truth for comparison: three reflectors were attached to the sample such that they could be measured with superordinate accuracy using the tracker.

Using SA the sample was scanned twice with a rigid movement of the entire sample in between. The transformation matrix modelling the rigid body movement was obtained from standard LT measurements to the reflectors. The point clouds C1 and C2 obtained from the two scans were then imported into the Geomagic software, where they were uniformly filtered to 0.1 mm. Several small patches were cut out of C1 and C2 (see Figure 11), only approximately covering the same area. Some of them were selected such that they have unique but diverse local surface structure (P1, P2, P3, P4). One mostly planar patch was selected (P7), and two patches (P5, P6) have surface geometry somewhere in between. As a first quantitative indication of surface texture, the RMS values of the points with respect to a best fit plane were computed for each patch. These values are given in Table 3. Generally, a higher RMS value suggests higher surface roughness; however, the variation of geometry can predominantly occur in one direction only thus fixing a degree of freedom in that particular direction, while not in the remaining directions. So, a high RMS value does not necessarily indicate that a patch is useful for this approach.

Using Geomagic the patches were independently registered with ICP, and the respective centre of gravity of each source patch was used as VMP. Transforming the coordinates of these points using the registration result yielded the coordinates in the respective second patch and thus the

estimated displacement vectors. The results are visualized in Figure 11 (right), and the deviations of the results from the ground truth are shown in Table 3 for a source patch size of $5 \times 5 \text{ cm}^2$. Smaller patches were also analysed but yielded significantly worse results.

The results indicate that displacement determination with sub-mm accuracy is possible using this approach, and the details visible in Table 3 agree well to the patch selection criteria mentioned above. We recognize that typically the uncertainty is lowest perpendicular to the dominant surface within each patch, while the matching fails in case of highly planar patches (P7). The accuracy seems to be also limited by the impact of steep edges which likely cause outliers within the point clouds or significant apparent changes with slight changes of the data acquisition geometry. Future research is needed to clarify these issues and identify surface patterns suitable for practical application at a larger scale.

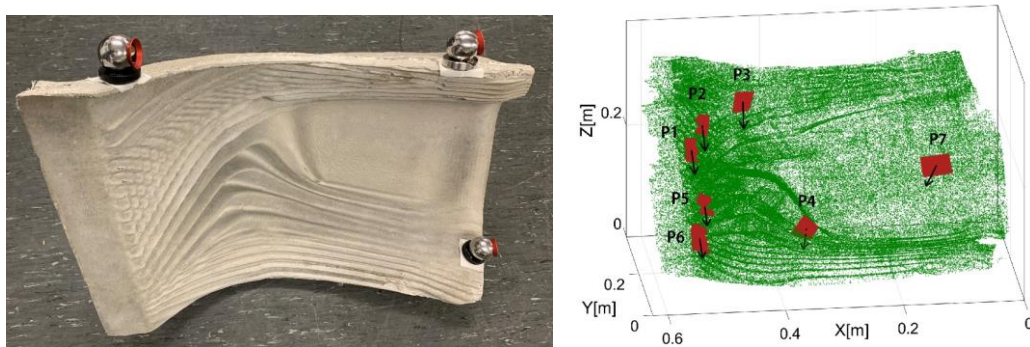


Figure 11: A section of the SmartSlab with attached reflectors (left) and displayed computed vectors with patches (right).

Table 3: Differences of patches translations with respect to the ground truth data and RMS of the plane fit to each patch.

	P1	P2	P3	P4	P5	P6	P7
Surface RMS [mm]	2.06	1.86	0.86	8.24	4.19	1.46	0.51
ΔX [mm]	0.85	-0.46	0.50	2.00	-0.93	-1.85	-12.48
ΔY [mm]	-0.15	0.10	0.14	-0.30	0.12	0.17	-1.41
ΔZ [mm]	0.47	0.18	-0.40	-0.44	3.95	0.51	104.29
$\Delta 3D$ [mm]	0.98	0.50	0.66	2.07	4.06	1.93	105.04

5. DISCUSSION

We presented the chosen solutions and selected results for geodetic monitoring of highly innovative digitally fabricated elements within a real building from shortly after the installation of the elements to the early use phase of the building. The elements are a very thin, highly structured concrete ceiling (SmartSlab), an S-shaped wall consisting of a metal mesh and sprayed concrete (MeshMould), and a timber framework (timber frame). Particular challenges were the limited knowledge about expected deformations both in terms of spatial and temporal patterns, the absence of parts known to be stable on the sub-mm level, and the limited permission to mount point markers on the structures to be monitored.

The solution therefore aimed at determining shape changes rather than displacements or deformations with respect to a fixed (external) reference coordinate system. Furthermore, we chose a combination of point-wise measurements using a LT and areal measurements using 3D laser scanners. The former allowed obtaining very high accuracy and sensitivity at selected points and thus detecting deformations at sub-mm level if they involve the monitoring points; the latter

allowed reducing the number of required point markers and obtaining nearly complete spatial coverage although with reduced sensitivity (mm-level).

The analyses show that the SmartSlab agreed with its design to within about 1.5 cm (maximum C2M deviations). Changes of less than 4 mm were found over the seven months monitoring period. Using the tracker and temperature measurements deformation patterns very likely related to temperature variations could be identified. MeshMould and timber frame, showed even smaller changes over time.

The VMP approach proposed herein, a hybrid approach combining the ideas of point-wise and areal monitoring, was tested in a lab experiment. Using a handheld scanner linked to the LT and a sample resembling a part of SmartSlab the applicability of this approach was demonstrated for detecting mm- or sub-mm level deformations.

The obtained results are a valuable contribution towards improving the related design and fabrication processes and demonstrating their technological readiness. The monitoring solution also helped assuring the safety of the structures for the users. Critical changes did not occur but would have been detected early enough for intervention. Further research is needed to exploit the potential of the VMP approach and possibly include it in the network analysis. This could facilitate point-wise measurements with sub-mm precision without markers on the structure.

6. ACKNOWLEDGMENTS

The measurements and analyses were financially supported by Siemens, Geberit, and the ETH Zürich Foundation upon approval by the Partnership Council Sustainable/Digital Construction. We thank Dr. Björn Niesen, DFAB House, EMPA for helping with access to the facility.

REFERENCES

Barnhart, T.B. and Crosby, B.T., 2013. Comparing two methods of surface change detection on an evolving thermokarst using high-temporal-frequency terrestrial laser scanning, Selawik River, Alaska. *Remote Sensing*, 5(6), pp.2813-2837.

Besl, P.J. and McKay, N.D., 1992, April. Method for registration of 3-D shapes. In *Sensor fusion IV: control paradigms and data structures* (Vol. 1611, pp. 586-606). International Society for Optics and Photonics.

Caspary, W., 2000. *Concepts of Network and Deformation Analysis* (Rüeger, JM, ed.). University of New South Wales, Sydney, Australia.

Chen, Y. and Medioni, G.G., 1991. Object modeling by registration of multiple range images. *Image Vision Comput.*, 10(3), pp.145-155.

Eling, D., 2009. *Terrestrisches Laserscanning für die Bauwerksüberwachung*. Leibniz-Univ., Fachrichtung Geodäsie und Geoinformatik.

Friedli, E. and Wieser, A., 2016. Identification of stable surfaces within point clouds for areal deformation monitoring. In *Proceedings of the 3rd Joint International Symposium on Deformation Monitoring (JISDM)*. Vienna, Austria. 30th March-1st April.

Gifftthaler, M., Sandy, T., Dörfler, K., Brooks, I., Buckingham, M., Rey, G., Kohler, M., Gramazio, F. and Buchli, J., 2017. Mobile Robotic Fabrication at 1: 1 scale: the in situ fabricator. *Constr Robot* 1 (1–4): 3–14.

Hack, N., Wangler, T., Mata-Falcón, J., Dörfler, K., Kumar, N., Walzer, A.N., Graser, K., Reiter, L., Richner, H., Buchli, J. and Kaufmann, W., 2017, March. Mesh mould: an on site, robotically fabricated, functional formwork. In *Second Concrete Innovation Conference (2nd CIC)*, Paper (No. 19).

Heunecke, O., Kuhlmann, H., Welsch, W., Eichhorn, A. and Neuner, H., 2013. *Handbuch Ingenieurgeodäsie. Auswertung Geodätischer Überwachungsmessungen*.

Kuhlmann, H., Schwieger, V., Wieser, A. and Niemeier, W., 2014. Engineering Geodesy-Definition and Core Competencies. *Journal of Applied Geodesy*, 8(4), pp.327-334.

Leica, 2017a. Leica absolute tracker AT960: Absolute Speed. Absolute Accuracy. Absolute Portability. Manual: Hexagon Metrology.

Leica, 2017b. Leica ScanStation P50. Manual: Leica Geosystems AG.

Meibodi, M.A., Jipa, A., Giesecke, R., Shammas, D., Bernhard, M., Leschok, M., Graser, K. and Dillenburger, B., 2018. Smart Slab. Computational design and digital fabrication of a lightweight concrete slab.

Neuner, H., Holst, C. and Kuhlmann, H., 2016. Overview on current modelling strategies of point clouds for deformation analysis. *AVN Allgemeine Vermessungs-Nachrichten*, 123(11-12), pp.328-339.

Niemeier, W., 1985. *Deformationsanalyse. Geodätische Netze in Landes-und Ingenieurvermessung II*, Kontaktstudium, ed. H. Pelzer, Wittwer, Stuttgart.

NRK, 2020. SpatialAnalyzer. New River Kinematics. Accessed 15.1.2020, kinematics.com.

Paffenholz, J.A. and Wujanz, D., 2019, May. Spatio-temporal monitoring of a bridge based on 3D point clouds-A comparison among several deformation measurement approaches. In *JISDM-Joint International Symposium on Deformation Monitoring* (pp. 15-17).

Pelzer, H., 1979. *Zur Analyse geodätischer Deformationsmessungen*. DGK, Reihe C, Nr. 164, München.

Raffl, L., Wiedemann, W. and Wunderlich, T., 2019. Non-signalized Structural Monitoring using Scanning Total Stations. In *4th Joint International Symposium on Deformation Monitoring*.

Renz, A., Solas, M.Z., de Almeida, P.R., Bühler, M., Gerbert, P., Castagnino, S. and Rothballer, C., 2016, May. Shaping the future of construction: A breakthrough in mindset and technology. In *World Economic Forum* (pp. 1-64).

Thoma, A., Adel, A., Helmreich, M., Wehrle, T., Gramazio, F. and Kohler, M., 2018, September. Robotic fabrication of bespoke timber frame modules. In *Robotic Fabrication in Architecture, Art and Design* (pp. 447-458). Springer, Cham.

Tsakiri, M., Lichti, D. and Pfeifer, N., 2006. *Terrestrial laser scanning for deformation monitoring*.

Van Gosliga, R., Lindenbergh, R., & Pfeifer, N. (2006). Deformation analysis of a bored tunnel by means of terrestrial laser scanning. ISPRS: Proceedings of the ISPARS Commission V Symposium, Dresden.

Wunderlich, T., Niemeier, W., Wujanz, D., Holst, C., Neitzel, F. and Kuhlmann, H., 2016. Areal deformation analysis from TLS point clouds—the challenge. Allgem. Verm. Nachr., 11/2016.

Z+F, 2017. Z+F IMAGER 5010. Manual: Zoller + Fröhlich GmbH.

BIOGRAPHICAL NOTES

VALENS FRANGEZ is a scientific assistant at the group of Geosensors and Engineering Geodesy (GSEG), Institute of Geodesy and Photogrammetry (IGP). In August 2019 he joined the NCCR Digital Fabrication as a doctoral researcher. His main interests are industrial metrology and machine vision for an in-line 3D shape determination and quality assessment of robotically fabricated structural elements.

EUGENIO SERANTONI is a scientific and teaching assistant at the group of Geosensors and Engineering Geodesy (GSEG), Institute of Geodesy and Photogrammetry (IGP). His interests include engineering geodesy, structural identification and monitoring, terrestrial laser scanning, and finite element modelling.

PROF. DR. ANDREAS WIESER is a full professor of Geosensors and Engineering Geodesy at ETH Zurich since 2012. He has held various academic positions at the Vienna University of Technology, Graz University of Technology and University of Calgary and worked as a product manager for GPS-based tolling in industry, before. His research interests are geodetic monitoring, digitization of reality, ubiquitous positioning, parameter estimation, and quality control.

CONTACTS

Valens Frangez
Geosensors and Engineering Geodesy
Institute of Geodesy and Photogrammetry
ETH Zürich
Stefano-Franscini-Platz 5, HIL D 46.2
CH-8093 Zürich
Tel. + 41 44 633 73 29
Email: valens.frangez@geod.baug.ethz.ch
Website: www.gseg.igp.ethz.ch